Even-Odd Effect of ^{35}Cl Quadrupole Coupling Constants in Solid *n*-Alkylammonium Chlorides (C_5 - C_{10})

H. Honda

Graduate School of Integrated Science, Yokohama City University, Kanazawa-ku,
Yokohama, 236-0027, Japan

Reprint requests to Dr. H. H.; E-mail: hhonda@yokohama-cu.ac.jp

Z. Naturforsch. **58a,** 623 – 630 (2003); received June 17, 2003

^{35}Cl NMR spectra were measured using the highest-temperature solid phase of $n\text{-}C_xH_{(2x+1)}NH_3Cl$ and $n\text{-}C_xH_{(2x+1)}ND_3Cl$ $(x = 5-10)$. The observed quadrupole coupling constants (e^2Qqh^{-1}) decreased upon heating in this phase, and significant frequency differences of *ca.* 20 – 30 kHz were detected between the -NH_3 and -ND_3 analogs. In the low-temperature range of this phase, the observed e^2Qqh^{-1} values for $x = 8, 10$ were larger than those for $x = 5, 7, 9$, which is attributable to the even-odd effect. Point-charge calculation was employed to explain this effect, in which the geometrical parameters and electric charge distributions of the cations were estimated using the B3LYP/6-31G* and B3LYP/6-31+G** method, respectively. The results show that the double-layer width between the Cl^- ions at the *2a* and *4f* sites strongly contributes to the e^2Qqh^{-1} value.

Key words: ^{35}Cl NMR Spectra; Theoretical Calculation of EFG; H-D Isotope Effect on Hydrogen Bonding; Even-Odd Effect.

1. Introduction

It is known that $n\text{-}C_xH_{(2x+1)}NH_3Cl$ (abbreviated as C*x*HCl) crystals ($x = 3 - 12$) can transform into the tetragonal phase with space group P4/nmn ($Z = 2$) at room temperature [1 – 4]. This highest-temperature solid phase (rotator phase) consists of a two-dimensional double-layer of lamella-type structure with the rod-like $n\text{-}C_xH_{(2x+1)}NH_3{}^+$ cations rotating about their long axes, and the Cl^- ions stacked alternately along the crystallographic *c*-axis. In low-temperature phases, on the other hand, cations with ordered orientations are intercalated with each other. The reported lengths on the *a*-axis in the rotator phase of these salts were comparable, while those on the *c*-axis increased nonlinearly with the carbon number. However, structural data on the single crystals of these rotator phases, except for C5HCl [3], are not available. To the best of our knowledge, the distances of NH—Cl and the positions of the Cl^- ions in a unit cell have not been reported. Even-odd effects have been detected in molecular crystals, in which the effect has been especially associated with the melting points of *n*-alkanes [5, 6]; however, the even-odd effects for ionic crystals have not been reported.

Solid-state ^{1}H and ^{2}H NMR studies have revealed the cationic 2-D self-diffusion in the lamella plane and the tumbling of the cationic long axis about the *c*-axis [7 – 14]. The temperature dependent ^{35}Cl quadrupole coupling constants (e^2Qqh^{-1}) were determined from solid-state NMR spectra of C4HCl [11]; the ^{35}Cl NQR frequencies were determined using the ^{1}H-^{35}Cl quadrupolar double resonance method for C6HCl [15], C8HCl [16], C10HCl [15, 17], and C10DCl [15]. To gain insight into the NH—Cl^- hydrogen bonding and characteristic structures in the rotator phase, together with the isotope effect due to the deuteration of ammonium groups, ^{35}Cl NMR spectra measurements for C*x*HCl and C*x*DCl ($x = 5 - 10$) were carried out in the rotator phase above room temperatures.

2. Experimental

C*x*HCl compounds were prepared by neutralizing liquid $n\text{-}C_xH_{(2x+1)}NH_2$ (Wako Pure Chemical Industries, Ltd.) with hydrochloric acid. Crude C*x*HCl crystals were obtained by adding ether to an aqueous solution, then recrystallizing from a solution of ether-ethanol 1:1. Partially deuterated analogs, $n\text{-}C_xH_{(2x+1)}ND_3Cl$ were obtained by repeated crystal-

0932–0784 / 03 / 1100–0623 $ 06.00

Table 1. Estimated values of e^2Qqh^{-1}/MHz from ^{35}Cl NMR spectra observed and reported for n-C$_x$H$_{(2x+1)}$NH$_3$Cl(CxHCl) and n-C$_x$H$_{(2x+1)}$ND$_3$Cl(CxDCl).

C5HCl	1.143±0.001 at 315 K		
C7HCl	1.401±0.001 at 300 K	C7DCl	1.375±0.001 at 300 K
C8HCl	1.501±0.001 at 315 K		
C9HCl	1.303±0.002 at 320 K	C9DCl	1.280±0.002 at 320 K
C10HCl	1.469±0.001 at 325 K	C10DCl	1.452±0.002 at 325 K
C4HCl [11]	1.21 at 300 K		
C6HCl [15]	1.45 at 330 K		

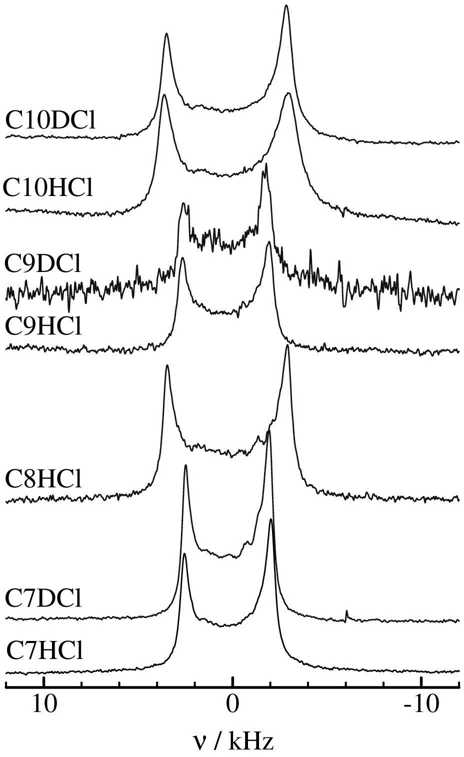

Fig. 1. ^{35}Cl NMR powder spectra of n-C$_x$H$_{(2x+1)}$NH$_3$-Cl(CxHCl) and n-C$_x$H$_{(2x+1)}$ND$_3$Cl (CxDCl) observed at 29.407 MHz and 360 K.

lizations (five times) from D$_2$O (99.9% deuterated, Aldrich Chemical Company, Inc.) under an atmosphere of dry N$_2$. The resulting crystals were annealed at 373 K for *ca.* 1 h.

^{35}Cl (I = 3/2) NMR spectra were measured at the Larmor frequency of 29.407 MHz using a Bruker MSL-300 spectrometer. Spectra were obtained from the echo signals observed after a $(\pi/2)_x-(\pi/2)_y$ pulse sequence. Crystalline NaCl was employed as the external reference of the ^{35}Cl chemical shift. The sample temperature was controlled and recorded using a Bruker VT-1000.

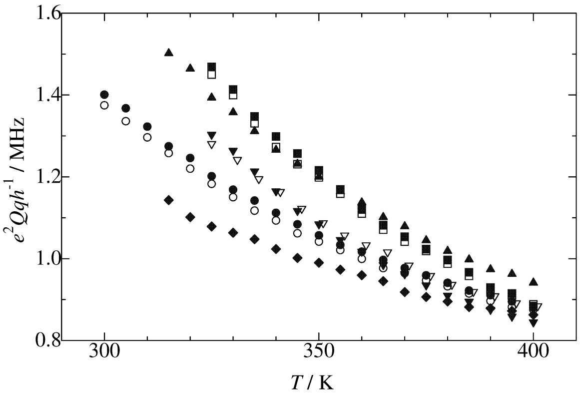

Fig. 2. Temperature dependent values of ^{35}Cl e^2Qqh^{-1}, estimated from the peak widths as shown in Fig. 1 for n-C$_5$H$_{11}$NH$_3$Cl (◆), n-C$_7$H$_{15}$NH$_3$Cl (●), n-C$_7$H$_{15}$ND$_3$Cl (○), n-C$_8$H$_{17}$NH$_3$Cl (▲), n-C$_9$H$_{19}$NH$_3$Cl (▼), n-C$_9$H$_{19}$ND$_3$Cl (▽), n-C$_{10}$H$_{21}$NH$_3$Cl (■), and n-C$_{10}$H$_{21}$ND$_3$Cl (□).

3. Result and Discussion

3.1. ^{35}Cl NMR Spectra of CxHCl and CxDCl

The ^{35}Cl NMR spectra for the central transition in the rotator phase of CxHCl and CxDCl are shown in Figure 1. The observed peak-widths became narrower with increasing temperature. Since the Cl$^-$ ions are located on the C_4-axis in this phase, the quadrupole coupling constant (e^2Qqh^{-1}) for $I = 3/2$ was evaluated using the relation [18]

$$\frac{e^2Qq}{h} = \frac{8}{5}\sqrt{3\Delta\nu^{(2)}\nu_L} \tag{1}$$

where eq, eQ, $\Delta\nu^{(2)}$, and ν_L are the electric field gradient (EFG), the quadrupole moment, the peak-width of the central transition, and the ^{35}Cl Larmor frequency, respectively. The temperature dependent e^2Qqh^{-1} values, estimated using (1), are shown in Fig. 2, which demonstrates the gradual decrease in the temperature gradients of e^2Qqh^{-1} with increasing temperature, and the dependence on the number of carbons. This result implies that the number of carbons determines the amplitude of the cationic thermal motion. The fact that large e^2Qqh^{-1} gradients were obtained for CxHCl with long carbon-chains is attributable to the larger vibration amplitude, resulting in higher averaged EFG at a

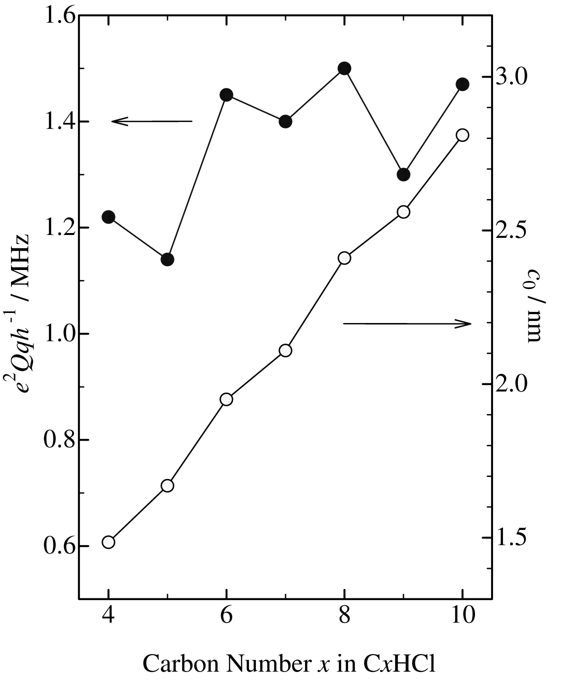

Fig. 3. Carbon number dependent e^2Qqh^{-1} values (●) and the reported crystallographic *c*-axis lengths (○) for *n*-$C_xH_{(2x+1)}NH_3Cl$ [1–3], where e^2Qqh^{-1} of *n*-$C_4H_9NH_3Cl$ and *n*-$C_6H_{13}NH_3Cl$ are reported values [11, 15].

Cl^- site.

For the deuterated analogs, the e^2Qqh^{-1} values shifted to slightly lower frequencies in the low-temperature range of the rotator phase, as shown on Table 1. These 17–26 kHz shifts, which are significantly greater than that of the experimental error of 1 kHz, are attributable to the isotope effect for the NH_3—Cl hydrogen bonds. This low-frequency shift can be explained as weaker hydrogen bonding as a result of the deuteration, since the vibration energies of D atoms forming H-bonds are lower than those of H atoms.

3.2. Even-Odd Effect of ^{35}Cl e^2Qqh^{-1}

As shown in Fig. 2, the e^2Qqh^{-1}-values for C8HCl and C10HCl were roughly comparable over the entire temperature range studied. In contrast, e^2Qqh^{-1} values for C5HCl, C7HCl, and C9HCl were clearly smaller than those of the above salts in the low-temperature range of this phase. An even-odd effect was observed for the e^2Qqh^{-1} values; for C6HCl at 300K, e^2Qqh^{-1} was 1.45 MHz [15], whereas lower values were obtained for C5HCl (1.40 MHz) and C7HCl (1.14 MHz). This even-odd effect was also found along the *c*-axis (Fig. 3); as the carbon number increased and alternated between even and odd, the increments in the *c*-length were smaller than the length of the CH_2 group. The packings of CxHCl with odd values of x were tighter than those with even values of x. Since it has been reported for *n*-alkanes [5, 6] that the packing energy of molecules with even number of carbons is lower than that with odd numbers, the even-odd effect obtained along the *c*-length was expected to be related with the difference in the packing energy caused by the cationic shape. The apparent even-odd effect of e^2Qqh^{-1} values can, therefore, be attributed to the relative packing of the cations and anions along the *c*-axis. Detailed discussions are presented in the subsequent section.

3.3. Point-Charge Calculation

Before considering the even-odd effect in EFG, the geometrical arrangements in the crystals will be discussed. Since two cations are contained in a unit cell of the rotator phase (space group: P4/nmn, $Z = 2$), as shown in Fig. 4(a), and since each cation rotates about its long axis along the C_4-axis, we define cation1 and cation2 as located along the C_4-axes and passing through (0,0,0) and ($a_0/2$, $a_0/2$, 0), respectively. The coordinates of C, H, and N atoms are expressed as (x_1, y_1, z_1) for cation1 and (x_2, y_2, z_2) for cation2. Since the cations rotate about their long axes, and the averaged structure adopts a rod-like shape as displayed in Fig. 4(b), the averaged positions of C, H, and N atoms in cation1 and 2 located on the C_4-axis are given by (0, 0, z_1) and ($a_0/2$, $a_0/2$, z_2), respectively. The Cl^-1 and Cl^-2 ions are placed at the *2a* and *4f* sites in a unit cell, respectively, *i.e.*, (0, 0, 0) and (a_0/2, a_0/2, z'), where z' is a general position. The anions are expected to form hydrogen bonds with both cation1 and 2, where the respective distances are represented by d_{11} and d_{12}. Using these parameters (Fig. 5), the position of N1 is expressed as (0, 0, d_{11}).

For the quantitative estimation of the Cl EFG values, point-charge model calculations were carried out. Since the reported N—Cl^- distance of 327 pm in C5HCl [3] indicates that the hydrogen bonding in CxHCl is relatively weak, and since the observed e^2Qqh^{-1} values are smaller than those of other compounds with short NH—Cl^- separations [19–30], the point-charge model can be accepted as a suitable approximation [31, 32]. Each component of the EFG for

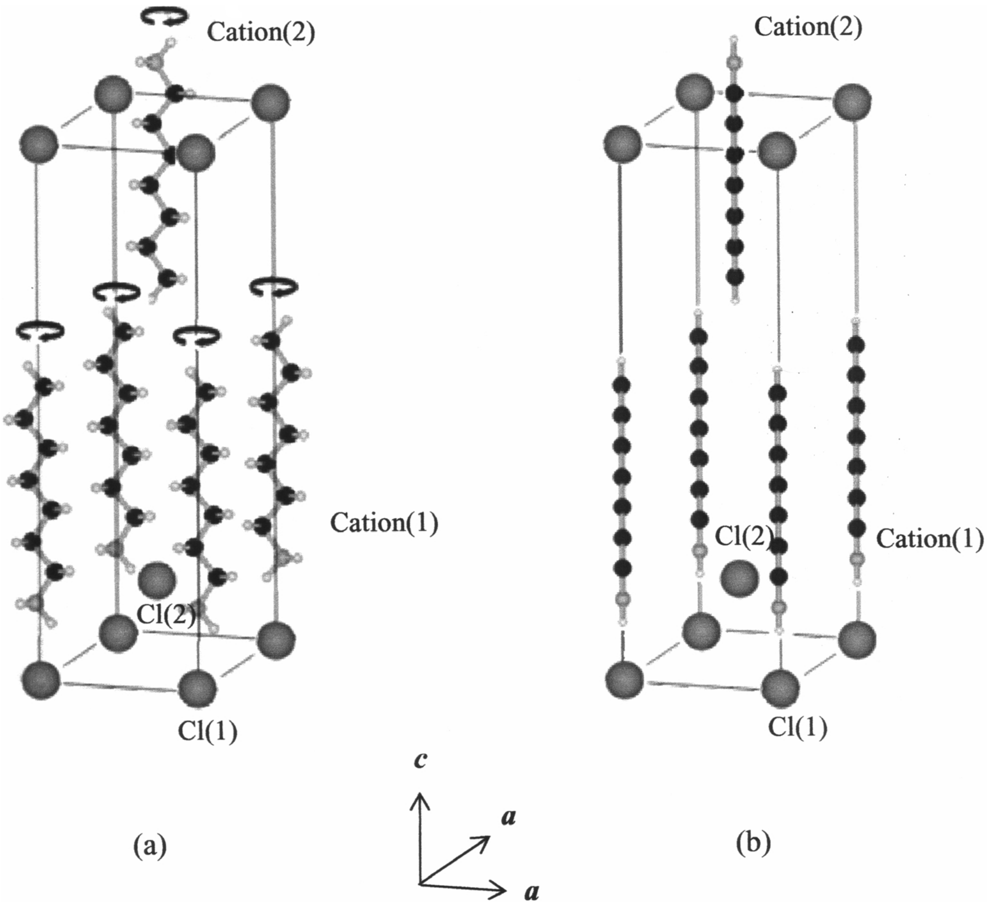

Fig. 4. (a) Atomic arrangements of n-C$_x$H$_{(2x+1)}$NH$_3$Cl crystals, in which the orientation of cation(1) and cation(2) are disordered about each C_4-axis. (b) Rod-like cation model used in the EFG calculation. The C, H, N atoms are placed on the C_4-axis.

the Cl$^-$ ion is expressed as

$$eq_{ij} = \sum_s c_s e \left(3\xi_{is}\xi_{js} - \delta_{ij} r_s^2\right) / r_s^5 \quad (i, j = x, y, z), \quad (2)$$

where ξ_{is}, δ_{ij}, r_s, and c_s are, respectively, the coordinates of the sth atom, Kronecker's δ, the distance between the Cl$^-$ ion and the sth atom, and the charge of the sth atom. The principal value of the EFG can be obtained by diagonalizing the quadrupole tensor given in (2). To calculate the coordinates and charges of the H, C, and N atoms in a rigid cation, the density function theory (DFT) in the Gaussian 98w program package [33] was employed. The B3LYP function with the 6-31G* basis set was used for the geometry optimization, and the same function with the 6-31+G** set was used to estimate the atomic charges. Calculated values of the charges are listed in Table 2. The use of a straight cation model indicated that the charges on the C, H, N atoms are concentrated on the C_4-axis.

In order to realize (2) for the crystal containing straight cations, two variables had to be introduced: d_{11}, which is the N1—Cl$^-$1 distance, and z', which is the z-coordinate of Cl$^-$2 forming a double-layer with Cl$^-$1 in the rotator phase. The coordinates of N1, Cl$^-$1, and Cl$^-$2 are expressed as (0, 0, d_{11}), (0, 0, 0), and ($a_0/2$, $a_0/2$, z'), respectively, as described above. In this system, two types of hydrogen bonds, N1—Cl$^-$1 and N1—Cl$^-$2, were formed, in which the latter distance, d_{12}, can be evaluated using d_{11} and z':

$$d_{12}^2 = \left(d_{11} - z'\right)^2 + \frac{a_0^2}{2} \quad (3)$$

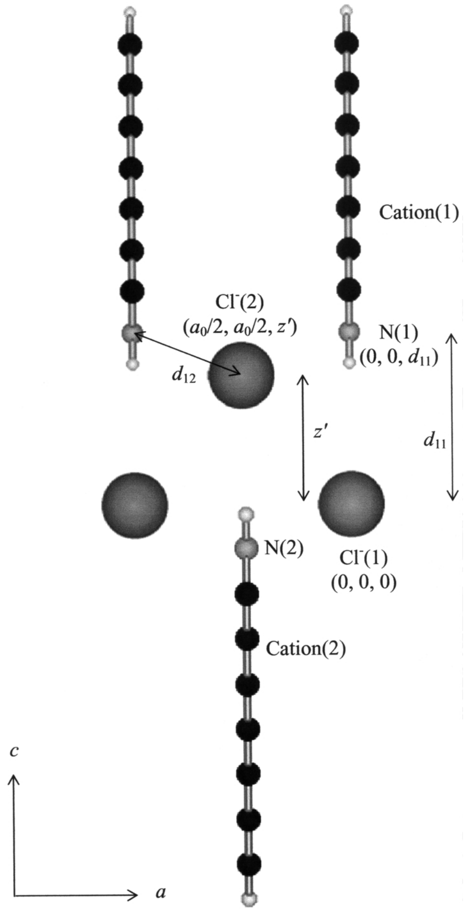

Fig. 5. Relative positions of N(1), N(2), Cl^-(1), and Cl^-(2) in the straight-cation model. The figure is projected on the *a*-*c* plane. The distances of N(1)—Cl^-(1) and N(1)—Cl^-(2), and the *z*-coordination of Cl^-(2) are represented by the symbols d_{11}, d_{12} and z', respectively.

Table 2. Atomic charges calculated for $n\text{-}C_xH_{(2x+1)}NH_3Cl$($CxHCl$). Atoms bonded to hydrogen are shown in parentheses. H_a and H_e denotes the hydrogen at the axial and equatorial positions, respectively.

Atoms	C5HCl	C6HCl	C7HCl	C8HCl	C9HCl	C10HCl
H_a (N)	0.4030	0.4032	0.4035	0.4038	0.4039	0.4041
N	−0.6030	−0.6005	−0.5994	−0.5993	−0.5992	−0.5996
H_e (N)	0.4016	0.4012	0.4012	0.4012	0.4011	0.4011
C_1	−0.1298	−0.1246	−0.1380	−0.1624	−0.1811	−0.2027
H_e (C_1)	0.2099	0.2098	0.2098	0.2096	0.2095	0.2094
C_2	−0.3259	−0.3636	−0.3620	−0.3861	−0.4088	−0.4242
H_e (C_2)	0.1638	0.1640	0.1639	0.1640	0.1641	0.1640
C_3	−0.2279	−0.1602	−0.1527	−0.1316	−0.1468	−0.1678
H_e (C_3)	0.1553	0.1558	0.1564	0.1562	0.1563	0.1563
C_4	−0.1324	−0.3037	−0.2403	−0.1970	−0.1551	−0.1493
H_e (C_4)	0.1480	0.1454	0.1457	0.1460	0.1458	0.1457
C_5	−0.6193	−0.1230	−0.3130	−0.2493	−0.1988	−0.1330
H_e (C_5)	0.1548	0.1449	0.1425	0.1428	0.1430	0.1428
C_6		−0.6344	−0.1217	−0.3176	−0.2612	−0.1982
H_e (C_6)		0.1511	0.1417	0.1391	0.1394	0.1396
C_7			−0.6555	−0.1336	−0.3521	−0.3072
H_e (C_7)			0.1494	0.1404	0.1380	0.1381
C_8				−0.6758	−0.1370	−0.3770
H_e (C_8)				0.1478	0.1390	0.1366
C_9					−0.6824	−0.1426
H_e (C_9)					0.1471	0.1385
C_{10}						−0.6901
H_e (C_{10})						0.1463
H_a (C_x)	0.1683	0.1623	0.1577	0.1547	0.1522	0.1506

To determine d_{11} and z' satisfying the experimental e^2Qqh^{-1} values, EFG calculations were carried out for $15 \times 15 \times 15$ unit cells with values of d_{11} and z' over the ranges $100 < d_{11} < 600$ pm and $-c_0/2 < z' < c_0/2$ pm. Using this process, the estimated principal values of the EFG were converged within ±10 Hz. Since the e^2Qqh^{-1} surfaces showing the relationship between d_{11} and z' and between d_{11} and d_{12} for C5HCl (shown in Fig. 6(a) and 6(b), respectively) were comparable to those for other salts, the EFG seems to be dependent on the chain length. The surfaces in Fig. 6 also indicate that the interaction between Cl^-1 and Cl^-2 strongly contributes to the EFG in a general range of $d_{11} > 270$ pm, because the maximum value of e^2Qqh^{-1} was obtained at $z' = 0$.

Using (2) and the reported values ($d_{11} = 327$ pm and $z' = 318$ pm [3]) together with the estimated parameters (Table 2), the value for e^2Qqh^{-1} was calculated as 0.102 MHz. However, the relatively small value as compared to the observed value of 1.143 MHz necessitated the consideration of the Sternheimer antishield factor (γ), which, in Cl, can adopt a wide range of values depending on the electronic structure around the nucleus [34]. The following equation for R_{x5} was therefore introduced for obtaining e^2Qqh^{-1} values without using γ for $CxHCl(x = 6-10)$:

$$R_{x5} = \frac{\left(e^2Qq_x\right)_{\text{exp}}}{\left(e^2Qq_5\right)_{\text{exp}}} = \frac{(1+\gamma)\left(e^2Qq_x\right)_{\text{calc}}}{(1+\gamma)\left(e^2Qq_5\right)_{\text{calc}}} \tag{4}$$

$$= \frac{\left(e^2Qq_x\right)_{\text{calc}}}{\left(e^2Qq_5\right)_{\text{calc}}},$$

where $(e^2Qq_5)_{\text{exp}} = 1.143$ MHz and $(e^2Qq_5)_{\text{calc}} = 0.102$ MHz. Values for R_{x5} were obtained for each CxHCl using experimental EFG values, $(e^2Qq_x)_{\text{exp}}$, in which the observed value at a temperature just above the phase transition to the rotator phase was taken to

Table 3. Estimated double-layer widths (*z'*) and -NH_3^+(1)—Cl^-(1) distances (d_{11}) in pm for each *n*-$C_x H_{(2x+1)}NH_3Cl$(C*x*HCl) from (4).

x	*z'*	d_{11}	*x*	*z'*	d_{11}
C5HCl [3]	318	327	C6HCl	309±3	327±23
C7HCl	317±3	328±20	C8HCl	310±3	328±23
C9HCl	320±5	326±30	C10HCl	311±3	328±23

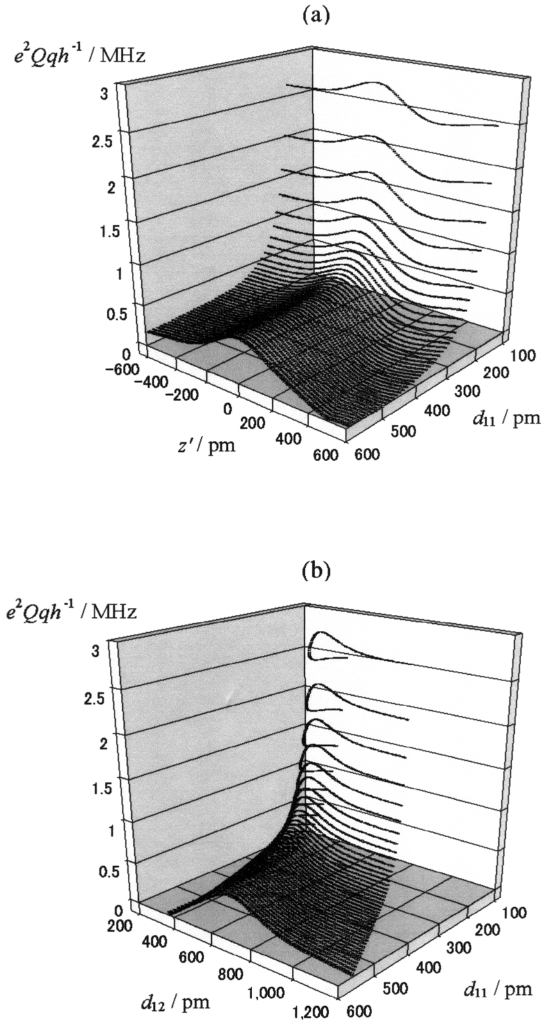

Fig. 6. Calculated e^2Qqh^{-1} surfaces of *n*-$C_5H_{11}NH_3Cl$ as functions of (a) the N(1)—Cl^-(1) distance (d_{11}) and the double-layer width (*z'*) where Cl^-(2) is located on ($a_0/2$, $a_0/2$, *z'*), and (b) N(1)—Cl^-(1) (d_{11}) and N(1)—Cl^-(2) (d_{12}) distances.

reduce the motional effect. Using (4), suitable combinations of d_{11} and *z'*, giving $(e^2Qq_x)_{\text{calc}}$, became available for each C*x*HCl. As shown in Table 3, the obtained *z'* values for C*x*HCl with odd values of *x* were larger than those with even values of *x* by *ca*. 10 pm. In contrast, the values for d_{11} were almost independent of *x*. These results are consistent with those displayed in Fig. 6, in which e^2Qqh^{-1} was significantly affected by *z'* rather than by d_{11} within the range $d_{11} > 270$ pm. A similar trend was observed for the X-ray studies of the iodide salts, C*x*HI(*n*-$C_xH_{(2x+1)}NH_3I$), where the *z'* values were estimated from the reported data of I^-1—I^-2 distances and the a_0-lengths of 341 ($x = 5$), 332 ($x = 6$), and 347 pm ($x = 7$) [3]. The results implied that the observed even-odd effects of e^2Qqh^{-1} correspond to the carbon number dependency of the double-layer width (*z'*) in C*x*HCl crystals. As shown in Fig. 7, the cationic reorientation about the principal axis of its moment of inertia can be proposed as a model that satisfies both the carbon number dependences of the double-layer width and the *c*-axis length. In this model, the two H atoms of -NH_3^+1 can form hydrogen bonds with Cl^-2 by the reorientation of -NH_3^+ about the rotational axis, as displayed in Fig. 7. Since the rotational axis that is apart from the N atom in the even carbon cations can result in a slightly larger arc that is defined by -NH_3^+, and in shorter -NH_3^+(1)—Cl^-2 distances, the -NH_3^+1 group in even carbon chains can be expected to form stronger hydrogen bonds than those in odd carbon chains. It can be suggested that these strong hydrogen bonds can partially neutralize the negative charge on Cl^-2, and thus decrease the electrostatic repulsion between Cl^-1 and Cl^-2, giving shorter *z'* for the even carbon chains.

3.4. Conclusion

^{35}Cl NMR spectrum measurements of C*x*HCl and C*x*DCl showed the H/D isotope effect and the even-odd effect of e^2Qqh^{-1}. To gain insight into the latter result, EFG calculations based on the point-charge model were carried out, in which the geometry and charges of the cation were estimated using B3LYP/6-31G* and B3LYP/6-31+G** methods, respectively. The results of these calculation indicated that the even-odd effects of e^2Qqh^{-1} correspond to the double layer width depending on the carbon number. Larger widths of the odd number chains than those of the even one are explained as the expected differences in the reorientation models of the cations.

Acknowledgement

The author is grateful to Prof. R. Ikeda and Dr. S. Ishimaru of University of Tsukuba for helpful dis-

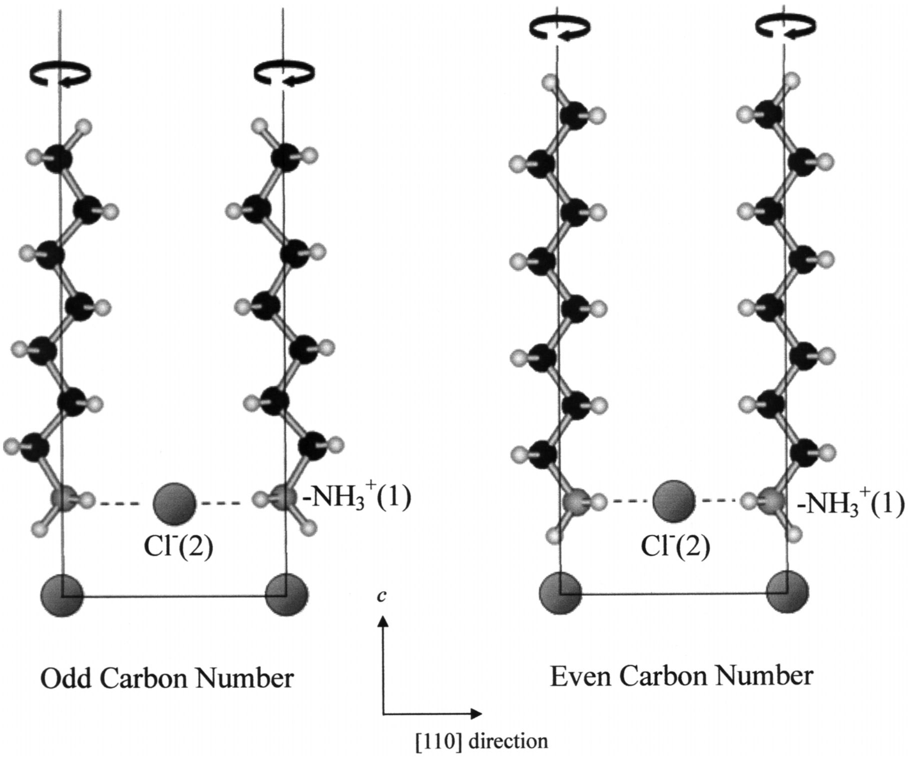

Fig. 7. A model of reorientation about the principle axis of the moment of inertia in the cations. The reorientation axis for the odd carbon cations is nearly on the N and -$\underline{C}H_3$ atoms, whereas, for the even carbon cations, the axis is apart from these atoms. The hydrogen bond between -NH_3^+(1) and Cl^-(2) is shown as a broken line.

cussion and the use of the MSL-300 spectrometer. This work was partly supported by the Grant in Support of Promotion of Research at Yokohama City University.

[1] S. B. Hendricks, Z. Kristallogr. **68**, 189 (1928); R. W. G. Wyckoff, Crytstal Structures, Wily Interscience, 2nd Ed., New York 1966, Vol. 5, Chapt. 14A.
[2] V. Busico, P. Cernicchiaro, P. Corradinl, and M. Vacatello, J. Phys. Chem. **87**, 1631 (1983).
[3] S. B. Hendricks, Z. Kristallographie **68**, 189 (1928).
[4] A. Terreros, P. A. Galera-Gomez, and E. Lopez-Cabarcos, J. Therm. Anal. Cal. **61**, 341 (2000).
[5] M. G. Broadhurst, J. Research of the National Bureau of Standards-A. Physics and Chemistry **66A**, 241 (1962).
[6] D. A. Pink, J. Chem. Phys. **63**, 2533 (1975).
[7] S. Fukada, H. Yamamoto, R. Ikeda, and D. Nakamura, J. Chem. Soc., Faraday Trans. 1, **83**, 3207 (1987).
[8] S. Iwai, R. Ikeda, and D. Nakamura, Can. J. Chem. **66**, 1961 (1988).
[9] M. Hattori, S. Fukada, D. Nakamura, and R. Ikeda, J. Chem. Soc., Faraday Trans. **86**, 3777 (1990).
[10] S. Iwai, M. Hattori, D. Nakamura, and R. Ikeda, J. Chem. Soc., Faraday Trans. **89**, 827 (1993).
[11] M. Hattori, Y. Onoda, T. Erata, M. E. Smith, M. Hattori, H. Ohki, and R. Ikeda, Z. Naturforsch. **49a**, 291 (1994).
[12] S. Tanaka, N. Onoda-Yamamuro, S. Ishimaru, and R. Ikeda, Bull. Chem. Soc. Japan **70**, 2981 (1997).
[13] Z. Fojud, C. Boeffel, E. Szczesniak, and S. Jurga, J. Mol. Struct. **555**, 107 (2000).
[14] E. C. Reynhardt and A. Wozniak-Braszak, Chem. Phys. Lett. **215**, 493 (1993).
[15] J. Seliger, V. Zagar, R. Blinc, R. Kind, H. Arend, G. Chapuis, K. J. Schenk, and F. Milia, Z. Phys. **B 69**, 379 (1987).
[16] J. Seliger, V. Zagar, R. Blinc, R. Kind, H. Arend, and F. Milia, Z. Phys. **B 67**, 363 (1987).
[17] J. Seliger, V. Zagar, R. Blinc, H. Arend, and G. Chapuis, J. Chem. Phys. **78**, 2661 (1983).
[18] M. H. Cohen and F. Reif, Solid State Phys. **5**, 321 (1957).
[19] G. A. Jeffrey and Y. Kinoshita, Acta Crystallogr. **16**, 20 (1963).

[20] E. J. Gabe and W. H. Barnes, Acta Crystallogr. **16**, 796 (1963).

[21] T. Ashida, S. Bando, and M. Kakudo, Acta Crystallogr. **B28**, 1560 (1972).

[22] R. Blinc, M. Mail, R. Osredkar, and J. Seliger, J. Chem. Phys. **63**, 35 (1975).

[23] P. K. Kadaba, J. Pirnat, and Z. Trontelj, Chem. Phys. Letters **93**, 382 (1975).

[24] M. Kurahashi, P. Engel, and W. Nowacki, Z. Kristallogr. **152**, 147 (1980).

[25] M. L. S. Garcia and J. A. S. Smith, J. Chem. Soc. Perkin Trans. II, 1401 (1983).

[26] C. H. Gorbitz, Acta Chem. Scand. **43**, 871 (1989).

[27] T. Erge, D. Michel, J. Petersson, and W. Windsch, Phys. Stat. Sol. (a) **114**, 705 (1989).

[28] T. Erge, F. Engelke, D. Michel, W. Windsch, and J. Petersson, Ferroelectrics **108**, 331 (1990).

[29] J.P. Yesinowski, M.L. Buess, A.N. Garroway, M. Ziegeweid, and A. Pines, Anal. Chem. **67**, 2256 (1995).

[30] D.L. Bryce, M. Gee, and R.E. Wasylishen, J. Phys. Chem. A **105**, 10413 (2001).

[31] A. Sasane, T. Matsuda, H. Honda, and Y. Mori, Z. Naturforsch. **47a**, 129 (1992).

[32] H. Honda, A. Sasane, K. Miyagi, A. Ishikawa, and Y. Mori, Z. Naturforsch. **49a**, 209 (1994).

[33] M. J. Frisch, G. W. Trucks, H. B. Schlegel, G. E. Scuseria, M. A. Robb, J. R. Cheeseman, V. G. Zakrzewski, J. A. Montgomery, Jr., R. E. Stratmann, J. C. Burant, S. Dapprich, J. M. Millam, A. D. Daniels, K. N. Kudin, M. C. Strain, O. Farkas, J. Tomasi, V. Barone, M. Cossi, R. Cammi, B. Mennucci, C. Pomelli, C. Adamo, S. Clifford, J. Ochterski, G. A. Petersson, P. Y. Ayala, Q. Cui, K. Morokuma, D. K. Malick, A. D. Rabuck, K. Raghavachari, J. B. Foresman, J. Cioslowski, J. V. Ortiz, B. B. Stefanov, G. Liu, A. Liashenko, P. Piskorz, I. Komaromi, R. Gomperts, R. L. Martin, D. J. Fox, T. Keith, M. A. Al-Laham, C. Y. Peng, A. Nanayakkara, C. Gonzalez, M. Challacombe, P. M. W. Gill, B. Johnson, W. Chen, M. W. Wong, J. L. Andres, C. Gonzalez, M. Head-Gordon, E. S. Replogle, and J. A. Pople, Gaussian 98, Revision A.6, Gaussian, Inc., Pittsburgh PA, 1998.

[34] E. A. C. Lucken, Nuclear Quadrupole Coupling Constants, Academic Press, London 1969, Chapt. 5.